Proceedings of the 5th ECPMG 2024
5th European Conference on Physical Modelling in Geotechnics
2-4 October 2024, Delft, the Netherlands

Centrifuge modelling of embankment overtopping

A.J. Bowman
Engineering Research and Development Center (ERDC), Vicksburg, MS, U.S., april.j.bowman@erdc.dren.mil

A.C. Trautz, J.W. Murphy, J. Westcott, C. Barela, R.S. Bockman
Engineering Research and Development Center (ERDC), Vicksburg, MS, U.S., andrew.c.trautz@erdc.dren.mil, john.w.murphy@erdc.dren.mil, joelle.a.westcott@erdc.dren.mil, clint.a.barela@erdc.dren.mil, ryan.s.bockman@erdc.dren.mil

ABSTRACT: The mechanisms which take place at the instant of dam overtopping leading to an eventual breaching and failure depend on many factors – breach dimension, time, soil conditions, reservoir size and inflow, and overflow depth are some of the many variables which contribute to the severity of overtopping failures in dams. Centrifuge tests can be beneficially used for parameter studies where material properties and behavior depend on both variation in boundary loads and conditions. To examine embankment overtopping a series of five centrifuge tests were conducted and compared to large scale testing conducted by Hanson et al. (2005). An examination of the scaling laws associated with time was performed comparing the width of headcut at the crest of the embankment between the two sets of data. Once a time factor is established an analysis of the erosion rate and cumulative volume loss was conducted.

1 INTRODUCTION

There are approximately 22,530 km of aging earthen embankments maintained by the US Army Corps of Engineers (USACE) across the United States (USACE, 2018). These structures are increasingly subjected to more frequent and extreme hydrologic loading events that could potentially lead to their failure and thus, subsequently pose significant flood risk to human life and property. One such failure mechanism, overtopping, has been attributed to 40% of earthen embankment failures in the last 70 years (Linsley and Franzini, 1979; Talukdar and Dey, 2019). Mathematically the process of overtopping is “an unsteady, nonhomogeneous, nonlinear, three-dimensional problem” which requires substantial understanding of soil-water interaction (Chow, 1959). It is dependent on a wide number of variables such as: embankment size and geometry, soil conditions (texture, moisture, compaction, etc.), and flood/overtopping depth (Talukdar and Dey, 2019). Current understanding of overtopping is primarily limited to a few historic post-failure investigations and small-scale, 1G experiments (e.g., Ellithy et al., 2018). The former provide no information on the processes occurring during active breaching and the latter have necessarily narrow scopes of work focused on only one or two variables of the problem. 1G-scale models fail to replicate the exact behaviour of the full-scale structure (also known as the prototype scale) due to the differing stress states under gravity loading.

Centrifuge testing is well-suited for studying overtopping failure as it allows the associated breaching process (i.e., erosion) to be observed, in real-time while ensuring model and the prototype similarity. Full-scale tests are cost prohibitive. Natural events are often remote, unpredictable, and lack instrumentation needed to conduct a comprehensive qualitative analysis. The feasibility of using centrifuge modeling in the context of overtopping was first demonstrated by Ko et al (1989) for two prototype embankments. More recent studies performed by Sun et al (2012), Zhao et al (2019), and Takahashi et al (2019) have explored various aspects of the problem. Irrespective of focus, these studies are corroborative in that they show centrifuge acceleration is necessary for producing the correct stress state, thereby adequately capturing the breaching process specific to scaled models. There are two primary objectives to this centrifuge study: (1) the continued improvement of the current understanding of overtopping failure by specifically looking at the relation between discharge, breach width, and eroded mass loss as a function of time; (2) development of an economical and repeatable testing approach for the USACE. The latter can greatly accelerate the R&D lifecycle while reducing the prohibitive costs, extensive logistical difficulties, and safety considerations required for full-scale testing. There is a lack of comprehensive, high-fidelity datasets at the appropriate stress state that can be used for numerical model development, calibration, and validation. Especially lacking in the literature is the rate of failure which is critical for understanding hazard to property and life downstream of an embankment. The centrifuge model design applied herein, specifically the soil properties, were based on that of the 1G experiments conducted by Hanson et al (2005). This was done to provide both a basis of comparison for the current study as well as to expand the existing dataset.

2 MATERIALS AND METHODS

The test design for these centrifuge models was driven by the desire to replicate the erosion processes observed in embankment overtopping tests conducted at the USDA-ARS Hydraulic Unit in Stillwater, Oklahoma (Britton et al., 2003). Hanson et al (2005) completed seven 1G overtopping tests on cohesive embankments ranging in height from 1.5 to 2.3 meters. These tests established a better framework of the erosion process seen during overtopping. Four stages, drawing from the work of Visser (1998), were described:

- Stage I: The initiation of overtopping flow (development of rill erosion) that results in the formation of a large headcut on the landward side of the embankment crest.
- Stage II: The migration of the headcut from the landward side to the water side of the embankment crest. The headcut begins to widen.
- Stage III: The embankment crest begins to erode and lower.
- Stage IV: The breach continues to widen while discharge continues until either the reservoir is drained or flood waters recede.

For this study, a series of five 25G centrifuge tests were conducted (see Table 1) at the Engineer Research and Development Center's (ERDC) Centrifuge Research Complex (CRC). The recently renovated 1,200 g-ton centrifuge has a 6.5m radius (Bowman et al., 2022).

Table 1. Centrifuge Test Matrix

Test Name	Soil Type	Density (g/cm^3)	Pretest Water Content (%)	Inflow (m^3/s)
Test 2	CL	1.78	9.3	1.8
Test 4	CL	1.72	11.6	1.4
Test 5	SM	2.02	7.5	2.7
Test 7	SM	1.84	7.2	2.4
Test 9[a]	SM	2.26	7.2	1.7

[a] Test's slope was 3:1; all other tests conducted with a 2:1 slope.

2.1 Model Design

Figure 1 shows the cross section design of the model set-up. In order to achieve steady flow conditions in the small space of the centrifuge box, the levee height in the centrifuge test was raised to 5 m (prototype) to increase the flow length down the face of the levee; the height of the Hanson et al. (2005) levees were 2.3 m (embankment 1) and 1.5 m (embankment 2). Given the lack of available full-scale datasets in the literature, the data from Hanson et al (2005) is used simply as a basis of comparison despite differences in the geometries. A self-priming impeller pump was used to control the water supplied to the model, creating discharge rates similar to those reported in the experiments of Hanson et al. (2005). The scaled levee was constructed on a raised platform and water was stored below this false bottom. A digital flow meter monitored the inflow which was controlled via a motor attached to the pump. Various catches to remove sediment suspended in the water were incorporated into the sytem. A large sediment catch basin was located downstream of the levee which prevented sizeable amounts of debris from interferring with the outflow. The outflow was determined by measuring the height of water as it flowed through a v-notched weir using miniture Pore Pressure Transducers (PPT) and correlated with video taken using a Raspberry Pi V2 camera placed directly in front of the v-notch weir. Additional PPTs were used throughout the model to measure water height above the crest, as well as pore pressure changes within the levee as a function of time.

The experiment design of this study was centered around the measurement of the breach formation, migration, and widening over time; this in turn, was used to determine erosion rate and total volume loss. An Intel RealSense D455 depth camera, mounted to the model container on the landward side of the levee, was used to measure surface elevation and geometery of any rills/gullies that formed. The D455 employs stereoscopic techniques to create depth maps that can be represented as a three-dimensional point clouds. Measurements have a depth accuracy of 2 mm. While the camera was used with great success in these experiments, it did have several negative characteristics. The camera was observed to be sensitive to changes in brightness/contrast of the model (e.g., water vs soil) and produced large file sizes that could prove unweildy to work with. In an effort to reduce file sizes, the camera was started and stopped several times throughout the experiments; this lead to unintentional shifts in the reference frame that had to be addressed during post processing.

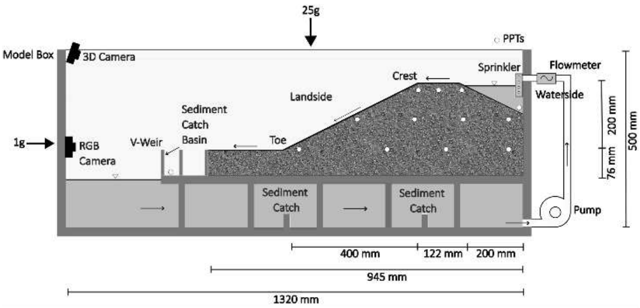

Figure 1: Layout in model scale 1

2.2 Soil Properties

In the Hanson tests three soils were tested, two non-plastic SM silty sand materials and a CL lean clay. The centrifuge work replicated the material properties of two of these soils. Key characteristics of the CL and SM soils manufactured for the centrifuge experiments are presented in Table 2.

Table 2. Soil Properties

Soil	**1**	**2**
Unified soil classification	CL	SM
Grain size distribution[a]		
% sand (40/70) > 0.75 mm	35	70
% silt (Vicksburg Silt) > 0.002 mm	40	25
% clay (Kaolin) < 0.002 mm	25	5
D_{50} (mm)	0.041	1.68
Atterberg Limits[b]		
Liquid limit	20.85	--
Plastic limit	12.7	--
Plasticity index	8.15	--
Compaction[c]		
Optimum water content (%)	10.2	7.3
Maximum dry density (g/cm^3)	1.93	2.02
Strength Characteristics[d]		
Friction Angle (degrees)	23.2	42.7
Cohesion (kPa)	33.1	24.5

[a] Measured according to ASTM standard D-422
[b] Measured according to ASTM standard D-4318
[c] Measured according to ASTM standard D-698
[d] Measured according to ASTM standard D-3080

The model embankment was constructed in lifts with a thickness of about 3 cm. The soils were compacted at optimum moisture content using a modified 10.6 kg drop hammer. In an effort to concentrate the flow and erosion to the center of the levee and away from the boundaries of the box, the crest was curved following the shape of the centrifuge‘s radial gravity field. All the models tested had the same geometry: a prototype height of 5 meters and landslide slope of 2:1, except Test 9 which had a slope of 3:1.

3 RESULTS AND DISCUSSIONS

A total of five tests were run as part of the current study, two with CL soil and three with the SM soil.

3.1 Breach Channel Formation

The erosion processes observed for each of these tests are presented in Figure 2 for the landward side of the levee crest. Analysis of the results show that the levees constructed from the CL soil were more resistant to erosion, visible in terms of the smaller rill/gully widths and depths. This is in good agreement with the reported findings of Hanson et al. (2005). The headcut geometry of each experimental realization of a given soil type is markedly different. Three channels formed in the case of CL Test 2 whereas only one was observed in CL Test 4. The width of the headcut of SM Test 5 was greater than that of SM Test 7 but the overall eroded depth was almost three times less. Collectively, these results show that small variability in soil properties, in this case bulk density, can have a profound impact on the evolution of breach rills/gullies.

3.2 Time Scaling

Subsequent analysis of the results i.e., erosion rate and mass loss require temporal consideration. Time scaling remains an open-ended question within the centrifuge modelling community. Surface deformation observed with the Raspberry V2 camera and D445 depth camera indicate that mass was lost from the levee due to erosion (i.e., channel cutting) as well as sloughing along the slope. These two mechanisms suggest that there are three possible ways to scale time from the model scale to the prototype scale. We considered three different time scales based on previous findings in the literature. Goodings (1984) reported that similarity requirements for erosion in a centrifuge model can be satisfied using a scaling factor of N. Gooding further reported that once sediment transport is fully established, the scaling factor becomes N^2, reflecting the turbulent nature of particle suspension in water. In recent work, Cabrera et al. (2020) suggest that a scaling factor of $N^{1/2}$ may be appropriate in cases of the occurrence of dry granular flows in centrifuges – directly applicable in cases of sloughing. It should be noted however that grain-fluid flows are not well understood (e.g., Goodings, 1984; Cabrera and Leonardi, 2022). Given the Hanson et al.

(2005) data is readily available for comparison, the associated temporal scaling of the centrifuge experimental results is explored herein; this is a necessary intermediate step that must be addressed prior to calculating erosion rate and mass loss as a function of time. Figures 3 and 4 compare the temporal evolution of breach widening measured by Hanson et al. (2005) and the centrifuge experiments of the present study. Note that the width of the breach is normalized to the maximum observed value in each

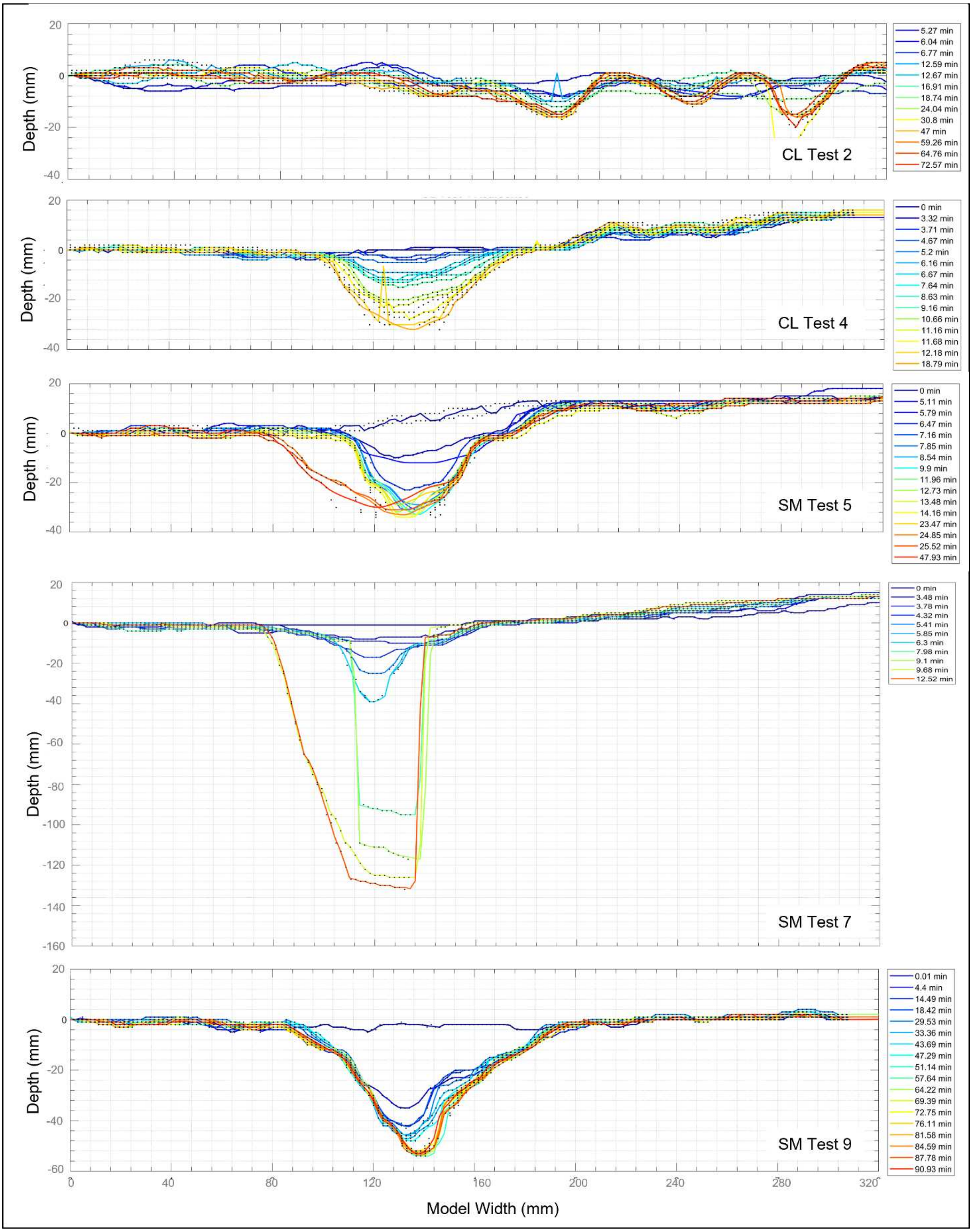

Figure 2. Centrifuge test cross sections 1

experiment; this was done to facilitate a direct comparison of both curve shape and overall magnitude. The three possible scaling factors discussed above were independently applied to the centrifuge results. CL Test 2 results were not included in the analysis (Figure 3) given the anomalous formation of three simultaneous head cut channels as such behaviour was not observed by Hanson et al. (2015).

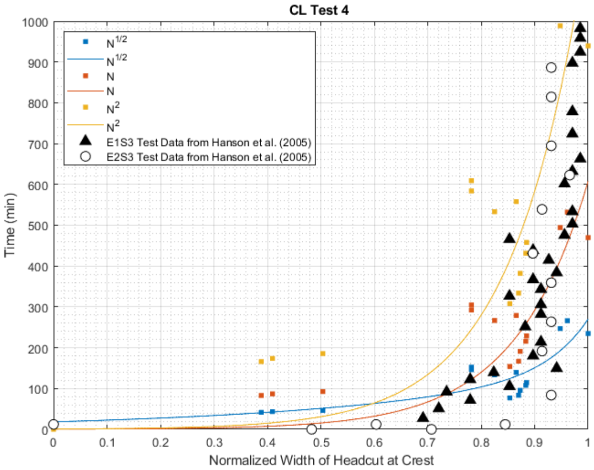

Figure 3. Comparison of centrifuge time scaling to Hanson et al (2005) data for CL soil.

Analysis of the results in Figures 3 and 4 suggest that all three scaling factors may be applicable, requiring that the soil type, current overtopping stage, and levee geometry all be considered.

In the case of the CL soil (Figure 3), scaling factors of N and N^2 provide the best fits to the Hanson et al. (2005) dataset. A scaling factor of N specifically corresponds well with the initial stages of overtopping (I-III) whereas N^2 is more relevant to Stage IV. These observations are in good agreement with Goodings (1984) who wrote that centrifuge time scaling of erosion can be described by a factor of N for the initiation of erosion and N^2 for full sediment transport. During the early stages of overtopping, a narrow channel will form and the discharge rate through the cut will be high per cross-sectional area basis; the associated high kinetic energy of the flow is sufficient for driving the erosion process. As the channel widens over time, the discharge rate per cross-sectional area decreases along with the associated kinetic energy of the flow. A slower scaling factor of N^2 therefore becomes more appropriate.

The results presented in Figure 4 show that scaling factors of N and N1/2 both provide good fits to the Hanson et al. (2005) data. N corresponded well to E2S1 and $N^{1/2}$ to E1S1 for SM Test 5 and SM Test 7, suggesting that the scaling factors could be used interchangeably. $N^{1/2}$ was the most appropriate scaling

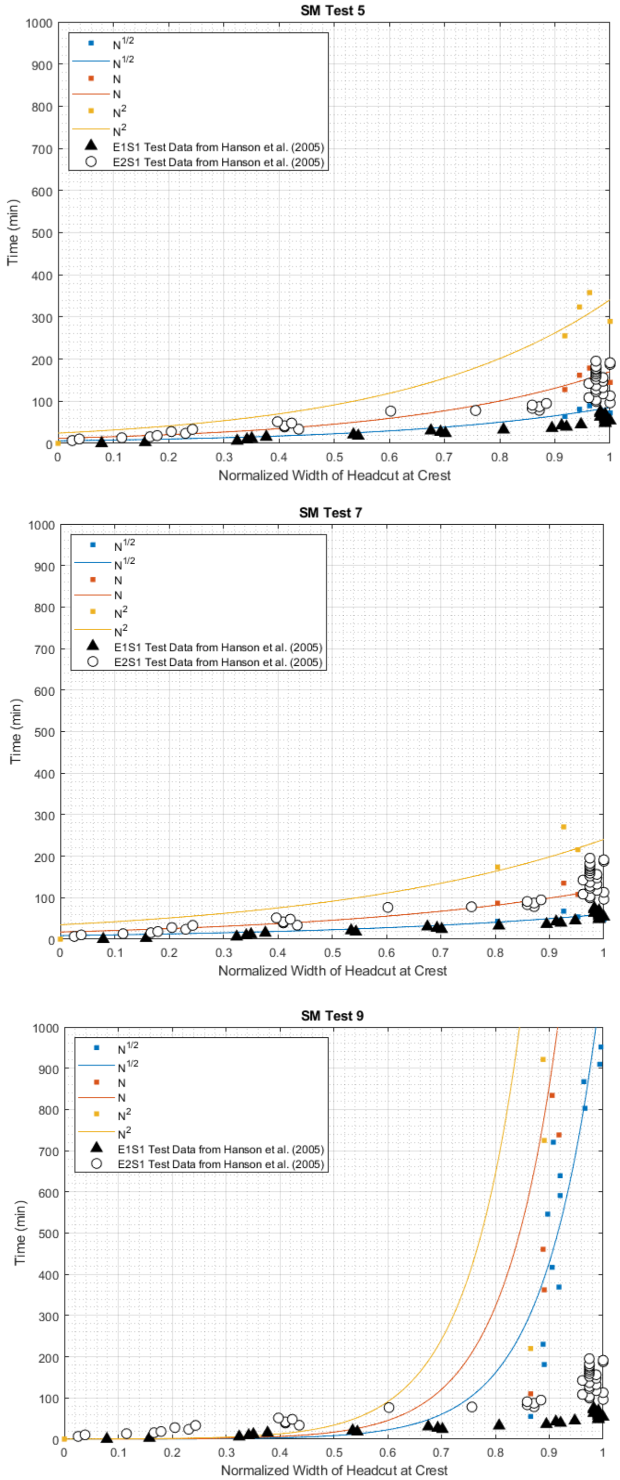

Figure 4. Comparison of centrifuge time scaling to Hanson et al (2005) data for SM soil.

factor in the case of SM Test 9; note that the fit to the Hanson et al. (2005) datasets is still poor. Much like the CL soil, a factor of N captures the process of erosion throughout the majority of the overtopping process (Goodings, 1984). Cabrera et al. (2020) posited that a scaling factor of $N^{1/2}$ may be appropriate of granular flow scenarios. This consideration is in good agreement with the sloughing behaviour observed in both the centrifuge models and Hanson et al (2005). In each experiment, the channel would widen suddenly as a large volume of soil would cleave and separate from the sides of the headcut. The scaling factor of $N^{1/2}$ therefore appropriately corresponds to shorter time duration.

While more model and prototype scale data is necessary to draw definitive conclusions regarding temporal scaling in this study, a factor of N will be used moving forward in the subsequent analysis given its applicability in the case of both the CL and SM soils over the majority of the overtopping stages.

3.3 Rate and Total Volume Loss

The total erosion rate observed during the breach widening process is presented in Figure 5 for each centrifuge experiment. These data were estimated by tracking the change in depth within the primary breach channel as a function of time from the cross-section data in Figure 2. A linear fit was in turn applied to these data to determine the erosion rate; note that this analysis was only applied to the datapoints corresponding to the active widening of the breach channel. The resulting total erosion rates are summarized in Table 3 along with the peak velocity calculated from the inflow flowmeter data.

The erosion rates and peak velocity data were next plotted (Figure 6) together following Briaud et al. (2008) to determine erosion classification. Results indicate that the SM tests can be classified as being of medium to high erodibility (II-III). The CL tests in contrast were classified as being of low erodibility (IV). These classes are consistent with the overall findings of Briaud et al. (2008). Class II-III erosion behaviour commonly corresponds to medium to coarse sands whereas Class IV is typical of high plasticity clays.

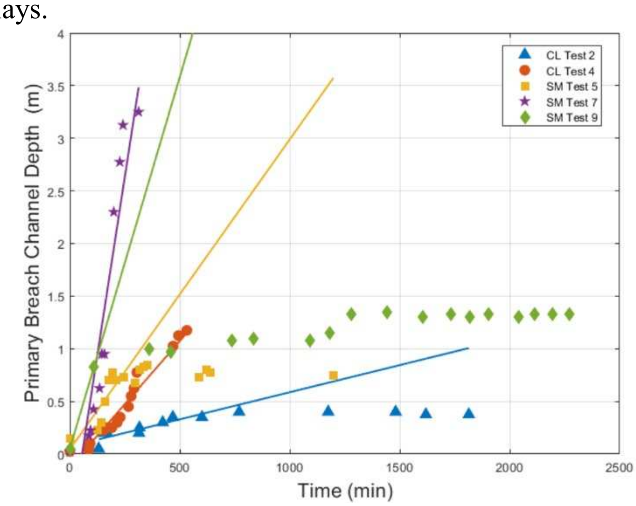

Figure 5. Erosion rate determined by tracing the depth of primary beach channel with time.

Table 3. Erosion Rates

Test Number	Peak Velocity (m/s)	Erosion Rate [mm/hr]
CL Test 2	27.2	30.8
CL Test 4	25.8	106.0
SM Test 5	6.0	194.2
SM Test 7	6.5	833.7
SM Test 9	0.87	437.5

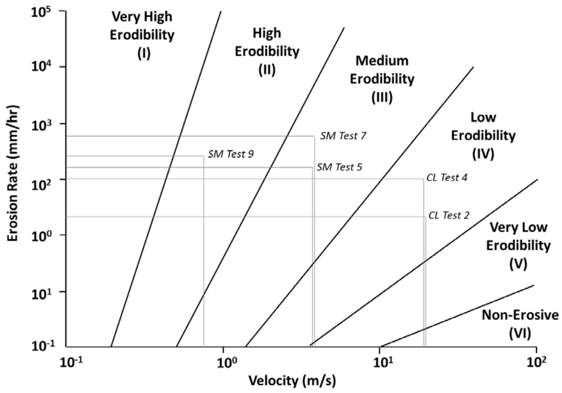

Figure 6. Erosion classification chart developed by Briaud (2008) with data from centrifuge tests indicated.

Finally, a total volumetric loss from the levee as a function of time was estimated for each centrifuge dataset (Figure 7), providing a quantitative assessment of the damage to the overall structure as a result of the overtopping failure. Volume loss was determined by integrating the point clouds measured by the D455 depth camera at multiple instances in time. This captured the increase in width and depth of the primary breach channel and any secondary rills/gullies that formed over the entire landward face of the levee. In general, the SM tests results presented in Figure 6 showed significantly more volume loss at a much higher rate, approximately two to three times more than the CL tests. The total volume losses for SM tests 5, 7, and 9 correspond to a 7.7, 9.2, and 5.2 percent

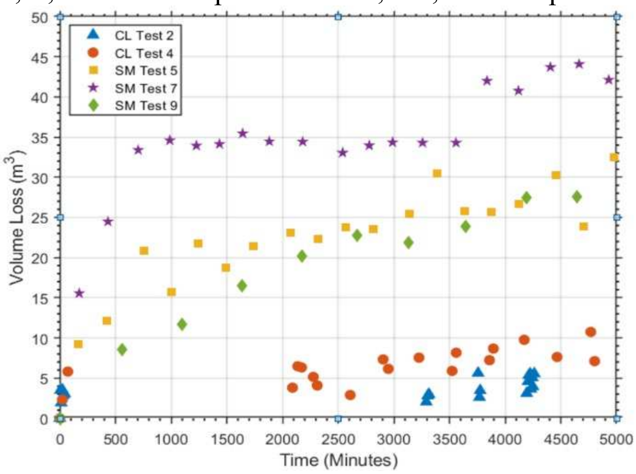

Figure 7. Estimated volume loss with time in levee section.

reduction in the overall volume of the original levee, respectively. Note that the total original volume of the levee in SM Test 5 was smaller than that of SM Test 9, hence the larger percent reduction in volume. Soil losses from CL Test 2 and 4 similarly corresponds to a 3.6 and 4.1 percent reduction in total levee volume.

4 CONCLUSIONS

Breaching failure because of overtopping is dependent on many factors including breach dimension, time, soil conditions, reservoir size and inflow, and overflow depth. The importance of these variables and the underlying processes remains poorly understood and limited primarily to a few post-failure investigations. Centrifuge modeling offers a unique alternative to expensive (logistically and financially) 1G experimentation.

The overall objective of this work was to conduct a series of controlled centrifuge experiments modelled after the 1G overtopping failure experiments of Hanson et al. (2005). The goal was to generate datasets that were complimentary and more expansive, incorporating cross-sections, erosion rate, and total volume loss analysis. Results of the centrifuge experiments, breach channel width evolution, were generally in good agreement with those of Hanson et al. (2005). The levees constructed out of SM soils were more susceptible to erosion and resulted in greater volumetric soil loss than the levees constructed from CL soils. The geometry and rate of erosion was also significantly more variable for the SM tests.

The dataset of Hanson et al. (2005) was furthermore extremely valuable from the perspective of centrifuge modelling in that it provided a basis of comparison necessary for exploring appropriate time scaling factors. It could be inferred from the analysis of the centrifuge experimental results, that a scaling factor of N was the most appropriate for the experiments. It should be noted that there remains considerable uncertainty regarding the validity of this conclusion with respect to soil type, overtopping stage, and levee geometry. Results were not as consistent with the 1G data as desired, suggesting that more testing of this nature is required.

ACKNOWLEDGEMENTS

The authors are grateful for the financial support provided by the US Department of Homeland Security and the technical support of the University of Mississippi.

REFERENCES

Bowman, A., Westcott, J., & Barela, C. (2022). History, Renovation and the Future of the Centrifuge Research Complex at the USACE ERDC. In *ICPMG 2022: 10th International Conference on Physical Modelling in Geotechnics*, 19-23 September 2022, Daejeon, Korea.

Briaud, J. L. (2008). Case histories in soil and rock erosion: Woodrow wilson bridge, brazos river meander, normandy cliffs, and new orleans levees. *Journal of Geotechnical and Geoenvironmental Engineering*, *134*(10), 1425-1447.

Britton, S. L., Hanson, G. J., & Temple, D. M. (2003). A historic look at the USDA-ARS hydraulic engineering research unit. In *Henry PG Darcy and Other Pioneers in Hydraulics* (pp. 263-276).

Cabrera, M. A., Leonardi, A., & Peng, C. (2020). Granular flow simulation in a centrifugal acceleration field. *Géotechnique*, *70*(10), 894-905.

Cabrera, M., & Leonardi, A. (2022). On the scaling principles of kinematic processes in a centrifugal acceleration field. In *Proceedings of the 10th International Conference on Physical Modelling in Geotechnics*.

Chow, V.T. (1959) Open Channel Hydraulics. McGraw-Hill Book Company. New York.

Ellithy, G.S., J.L. Wibowo, and M.K. Corcoran. (2018) Erosion rate equations for coarse-grained materials using a small flume testing. Scour and Erosion IX (pp.525-530). DOI: 10.1201/9780429020940-71

Goodings, D. (1984). Geotechnical centrifuge modeling of soil erosion. *Transportation Research Record*, *998*(1).

Hanson, G. J., Cook, K. R., & Hunt, S. L. (2005). Physical modeling of overtopping erosion and breach formation of cohesive embankments. *Transactions of the ASAE*, *48*(5), 1783-1794.

Ko, H. Y., Dunn, R. J., & Hollingsworth, T. (1989). Study of Embankment Performance during Overtopping and Throughflow. Report 3. Model-Prototype Comparison Studies. Colorado University at Boulder.

Linsley, R. K., and Franzini, J. B. (1979). *Water-resources engineering*, McGraw-Hill, New York

Leonardi, A., Cabrera, M. A., & Pirulli, M. (2021). Coriolis-induced instabilities in centrifuge modeling of granular flow. *Granular Matter*, *23*, 1-8.

Sun, E., Zhang, X., Li, Z., & Wang, Y. (2012). Tailings dam flood overtopping failure evolution pattern. Procedia Engineering, 28, 356-362.

Takahashi, H., Morikawa, Y., Mori, N., & Yasuda, T. (2019). Collapse of concrete-covered levee under composite effect of overflow and seepage. Soils and Foundations, 59(6), 1787-1799.

Talukdar, P., & Dey, A. (2019). Hydraulic failures of earthen dams and embankments. *Innovative Infrastructure Solutions*, *4*, 1-20.

U.S. Army Corps of Engineers. (2018). *Levee Portfolio Report*. U.S. Army Corps of Engineers Levee Safety

Zhao, T., Chen, S., Fu, C., & Zhong, Q. (2019). Centrifugal model tests and numerical simulations for barrier dam break due to overtopping. Journal of Mountain Science, 16(3), 630-640.